2015 IEEE International Conference on Robotics and Automation (ICRA)
Washington State Convention Center
Seattle, Washington, May 26-30, 2015

Whole-Body Multi-Modal Semi-Autonomous Teleoperation of Mobile Manipulator Systems

ChangSu Ha[1], Sangyul Park[1], Jongbeom Her[1], Inyoung Jang[1], Yongseok Lee[1], Gun Rae Cho[2], Hyoung Il Son[3], and Dongjun Lee[1†]

***Abstract*— We propose a novel whole-body multi-modal semi-autonomous teleoperation framework for mobile manipulator systems, which consists of: 1) Motion capture and whole-body motion mapping to allow the operator to intuitively teleoperate the mobile manipulator without being constrained by the master interface while also fully exploiting whole-body dexterity; 2) Slave robot autonomous control to allow the mobile manipulator to optimally track the operator's whole-body command, while taking into account the user-slave kinematic dissimilarity (slave robot's joint limit, joint velocity limit, and singularity); and 3) Visuo-haptic-vestibular feedback with HMD (Head Mounted Display) for 3D visual information, wearable cutaneous haptic device for manipulation force feedback, and actuated chair for vestibular feedback to reduce HMD-induced motion sickness. Performance of the proposed framework is validated with simulation of a ROV (remotely operated vehicle) manipulator system and some preliminary user studies.**

I. Introduction

Even with the recent substantial advancements in technology for autonomous robotic operations, for many real-world robotic tasks, it is still challenging (and often impossible) to perform the task in a complete autonomous fashion, particularly when the task takes places in unstructured, uncertain and dynamic environments. For such real-world tasks in unstructured/dynamic environments, teleoperation is often the only viable solution, where human can solve many crucial tasks (e.g., remote manipulation even with fairly limited information, navigation/operation in unstructued/unmapped environment with dynamic obstacles, etc.). These tasks are typically very difficult or even impossible to be addressed by fully-autonomous robots.

Due to this importance, telerobotics has been one of the main research areas in the robotic community and has enjoyed many strong results, particularly for the interaction stability problem of bilateral teleoperation with or without communication imperfectness (e.g., [1], [2], [3], [4], [5]). Yet, the wide adoption of advanced telerobotic systems for complex slave robots in real-world applications has been rather slow.

[1]: Department of Mechanical & Aerospace Engineering and IAMD, Seoul National University, Seoul, Republic of Korea, 151-744. Email: {changsuha,sangyul,jongbeom.her,yongseoklee,iyjang,djlee}@snu.ac.kr
[2]: Mechatronics Center, Samsung Heavy Industries CO., LTD, Daejeon, Republic of Korea, 305-380. Email: gunrae.cho@samsung.com
[3]: Department of Rural and Biosystems Engineering, Chonnam National University, Gwangju, Republic of Korea, 500-757. Email: hison@jnu.ac.kr
† Corresponding author: djlee@snu.ac.kr
Research supported in part by the Global Frontier R&D Program on 'Human-centered Interaction for Coexistence'(NRF-2013M3A6A3079227), the Basic Science Research Program (2012-R1A2A2A0-1015797), and the Brain Korea 21 Plus Project in 2014 (F14SN02D1310) of the National Research Foundation (NRF) by the Korea Government (MEST) and Samsung Heavy Industries.

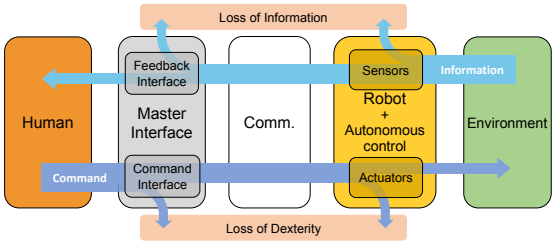

Fig. 1: Dexterity loss and information loss in telerobotic systems through the master interface and the slave robot with limited sensing and actuations.

This we believe is because the current telerobotics technologies are somewhat not so able to fully compensate for the two main issues of teleoperation: **loss of dexterity and loss of information.** More precisely, from Fig. 1, as compared to the case of direct human manipulation with dexterity and rich on-site information, we can see that: 1) the human dexterity will be compromised by the kinematic/dynamic constraints of the master device (e.g., kinesthetic device with small degree-of-freedom (DOF) and large inertia/friction) and also due to the restricted dexterity of the slave robot, which can be further exacerbated by improperly-designed local slave control; and 2) the rich information at the slave side will be lost due to the limited sensing of the slave robot (e.g., typically no tactile feedback, although human hand/finger has numerous mechanoreceptors) and also further compromised due to the lack of actuation/display of the master interface (e.g., no force feedback with monocular camera-feed for typical ROV teleoperation).

In this paper, we propose a novel whole-body multi-modal semi-autonomous teleoperation framework for mobile manipulator systems with the aim to minimize these dexterity loss and information loss. Our proposed teleoperation system consists of the following components:

- **Motion capture and whole-body motion mapping** to contactlessly measure the whole-body motion of the operator and map this into the slave mobile manipulator, so that the operator can intuitively tele-command the mobile manipulator without being hindered by kinematic/dynamic constraints of the master interface, while also fully exploiting their whole-body dexterity;
- **Slave robot autonomous control** to allow the slave mobile manipulator to faithfully track the whole-body command of the operator, while taking into account the kinematic dissimilarity (slave robot's joint limit, joint velocity, and singularity) between human user and slave

robot with priority placed on certain subsets of the slave motions, which are more important for usability;

- **Visuo-haptic-vestibular feedback**, in which high-quality 3D visual information[1] is provided by a HMD (Head Mounted Display), haptic feedback is provided by the cutaneous haptic device [6], [7], and vestibular feedback is provided by actuated chair to reduce motion sickness due to the sensory conflict [8] associated with the use of HMD. See Fig. 2.

In contrast to the abundance of results on the teleoperation of manipulators, results on the teleoperation of mobile robots or mobile manipulator are relatively rare, e.g., mobile robots [9], aerial robots [10], [11], [12], [13], mobile manipulators [14], [15]. Yet, all those results do not explicitly aim to minimize the dexterity loss and the information loss of telerobotic systems as we attempt to here, with all of them either utilizing only kinesthetic interfaces (with limited-DOF) instead of the operator's whole-body dexterity (e.g., [9], [10], [11], [12], [14], [15]); or focusing only to kinesthetic haptic feedback (e.g., [9], [10], [11], [12], [15]) or even completely missing any haptic feedback (e.g.,[13], [16]) in contrast to our visuo-haptic-vestibular feedback.

Our proposed multi-modal whole-body teleoperation framework is in fact inspired by the seminal work of "Tele-existence" [17], which has been recently evolved into the teleoperation system of the humanoid robot "TELESAR V" [18], with the contact-less human motion capture and cutaneous haptic device as we also utilize in this paper. However, these results [17], [18] are limited to anthropomorphic slave robots and the issue of significant kinematic dissimilarity, which is prominent for the mobile manipulator teleoperation with the moving platform, was not considered therein. Another related multi-modal teleoperation systems were proposed in [19], [20], which however were still limited to anthropomorphic slave robots and also, with their adoption of exo-skeleton type kinesthetic master interface, suffered from the loss of human dexterity due to the kinematic/dynamic constraints imposed by the exo-skeleton. Vestibular feedback, which we found to be important to reduce the HMD-induced motion sickness, was not considered either in [17], [18], [19], [20] (except for the mobile master interface of [19]).

The rest of the paper is structured as follows. System modeling is given in Sec.II. Our multi-modal whole-body semi-autonomous teleoperation framework is then presented in Sec. III with details about each component design. Experiment result and some preliminary user study result are given in Sec.IV, and Sec. V concludes the paper concludes with summary and comments on future research.

II. System Modeling

A. The Frames and Kinematic Relations

To describe the pose of the human user and the slave robot, we define the following coordinate frames: 1) the ground fixed inertial frame $\{\mathcal{I}\}$ for the human and $\{\mathcal{O}\}$ for the slave;

[1]Here, we include this visual information, as we believe it is crucial for manipulation tasks, perhaps, at least as important as haptic feedback. Note that remote manipulation is still possible only with monocular camera-feed in many ROV operations.

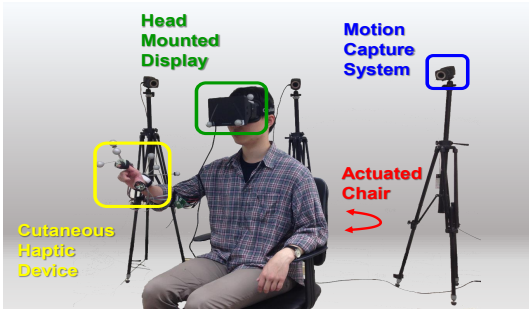

Fig. 2: Master interface: motion capture system to contactlessly measure whole-body motion, HMD and cutaneous haptic device to deliver 3D visual information and grasping force feedback, and actuated chair to reduce HMD-induced motion sickness.

2) the human torso-fixed frame $\{\mathcal{B}\}$ and the ROV platform-fixed frame $\{\mathcal{R}\}$; 3) the human head (and HMD) frame $\{\mathcal{E}\}$ and the ROV's camera frame $\{\mathcal{C}\}$; and 4) the human hand and finger frames, $\{\mathcal{H}\}$ and $\{\mathcal{F}\}$, and the ROV manipulator's end-effector frame, $\{\mathcal{T}\}$. See Fig. 3. On top of these, we also define $\{\mathcal{D}\}$ to be rigidly attached to the actuated chair, which will be used later.

Among any two of these frames, we can then define $SE(3)$ transformation, e.g., between $\{\mathcal{A}\}$ and $\{\mathcal{B}\}$:

$$g_{ab} := \{(q_{ab}, R_{ab}) : \ q_{ab} \in \Re^3, R_{ab} \in SO(3)\}$$

where q_{ab} is the position vector of the origin of $\{\mathcal{B}\}$ from the origin of $\{\mathcal{A}\}$ expressed in $\{\mathcal{A}\}$ and R_{ab} is the orientation of $\{\mathcal{B}\}$ relative to $\{\mathcal{A}\}$ expressed in $\{\mathcal{A}\}$. If $\mathcal{A}$ and $\mathcal{B}$ are same, $q_{ab} = [0;0;0]$ and $R_{ab} = I$. Let us also recall the body velocity between $\{\mathcal{A}\}$ and $\{\mathcal{B}\}$ as defined by

$$V^b_{ab} := \begin{bmatrix} v^b_{ab} \\ \omega^b_{ab} \end{bmatrix} = \begin{bmatrix} R^T_{ab}\dot{q}_{ab} \\ (R^T_{ab}\dot{R}_{ab})^\vee \end{bmatrix} \ \in \ \Re^6$$

where v^b_{ab}, w^b_{ab} are the translation and angular velocities of $\{\mathcal{B}\}$ relative to $\{\mathcal{A}\}$ expressed in $\{\mathcal{B}\}$ and $\vee$ is the operator to map a skew-symmetric matrix to its corresponding vector.

B. ROV-manipulator System

As an example of mobile manipulators, in this paper, we consider a ROV-manipulator system, which consists of a mobile platform evolving in $SE(3)$ and actuated by eight thrusters and a 6-DOF manipulator attached to the front of the ROV. A pan-tilt camera is also rigidly-attached to the front side of the ROV with no translation between the ROV and the camera (i.e., $\dot{q}_{rc} = 0$ although $w^b_{rc} \neq 0$). See Fig. 3. For this paper, we also assume that the ROV-manipulator system is equipped with an adequately-functioning low-level controller, with which we can achieve desired rates for each joint of the manipulators and desired translation/angular velocities of the ROV simultaneously. This may be possible by designing the ROV control law to be robust against the disturbance produced by the manipulator motions by using its redundant actuations (e.g., [21], [22]). See also [23] for dynamic control of general vehicle-manipulator systems.

With the low-level control, we can then consider the translational and rotational velocity of the ROV, the rates of each of the manipulator joints, and the angular rates of the ROV camera angular velocity as our control inputs u for

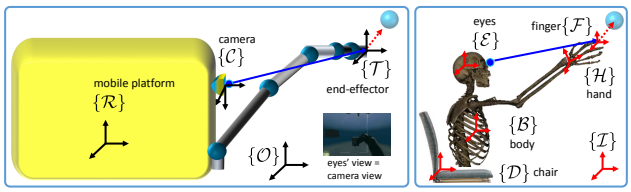

Fig. 3: Assignment of frames for whole-body teleoperation: four frames ($\{\mathcal{O}\}, \{\mathcal{R}\}, \{\mathcal{C}\}, \{\mathcal{T}\}$) for the ROV and five frames ($\{\mathcal{I}\}, \{\mathcal{B}\}, \{\mathcal{E}\}, \{\mathcal{H}\}, \{\mathcal{F}\}$) for the human user, who sees the slave site via the camera $\{\mathcal{C}\}$ of the ROV through HMD.

the slave mobile manipulator, that is,

$$u := \begin{bmatrix} V_{or}^b; & \omega_{rc}^b; & \dot{\theta} \end{bmatrix} \in \mathfrak{R}^{6+3+n} \tag{1}$$

where ω_{rc}^b is the camera angular velocity expressed in $\{\mathcal{C}\}$ and $\dot{\theta} := [\dot{\theta}_1; \cdots; \dot{\theta}_n] \in \mathfrak{R}^n$ is the collection of all the joint rates of the manipulator.

III. Multi-Modal Whole-Body Semi-Autonomous Teleoperation Framework

In this section, we explain our proposed teleoperation framework, consisting of the whole-body motion mapping with motion capture system, the slave robot autonomous control, and the visuo-haptic-vestibular feedback design.

A. Whole-Body Teleopeartion Command Mapping

Since the ROV-manipulator consists of the parts which have similar function to the human's (e.g. manipulator and human arm), one way through which the human user can intuitively operate the slave robot is to map the motion of human user onto the motion of the corresponding parts of the mobile manipulator. For instance, we can map the human head motion (i.e. HMD) onto the ROV's camera motion so that if the operator rotates his/her head to look around, camera view should be changed in response to the head motion. Similarly, we can connect the human torso motion to the ROV body motion, and hand motion to the end-effector motion. More detailed explanation of this whole-body motion mapping is given below.

1) Head vs. Camera: The ROV's camera view should be changed as the master rotates his/her head. Thus, the objective is to match the two rotations, R_{rc} and R_{be}. In other words, the ROV camera should move to achieve the following objective:

$$R_{rc} \rightarrow R_{be} \tag{2}$$

2) Torso vs. ROV: Although the human body and ROV-manipulator systems has some correspondence between their motions, their workspaces have different ranges as the human user is seated on the actuated chair, whereas the ROV is a mobile platform. Thus, we adopt the position-velocity mapping for translational motion command. Moreover, since the operator can only rotate their torso (by bending or twisting the waist) on the chair (See, Fig. 4), we should map the $SO(3)$ motion of the human torso to the $SE(3)$ motion of the ROV.

We assume that the user's intention to drive the ROV is reflected by their torso motion. More precisely, if the user leans his body forward while looking forward during grasping task (See, (a) in Fig. 4), we interpret this motion to imply that the user wants to move further forward because an object is too far to reach with their arm (so, the ROV should translate in the same direction). On the other hand, if the user bends at the waist 'while looking down' (See, (b) in Fig. 4), we interpret this motion to indicate that the user wants to rotate the entire ROV to capture the bottom view due to the limitation of the ROV camera's viewing range. Similar to the previous cases, we map the user's twist motion (See, (c) in Fig. 4) onto the ROV's rotational motion (yaw rotation), and sideward torso motion (See, (d) in Fig. 4) to the ROV's sway to the side direction. Note that we can distinguish two similar motions (a) and (b) by measuring the orientation of the user's head (i.e. HMD).

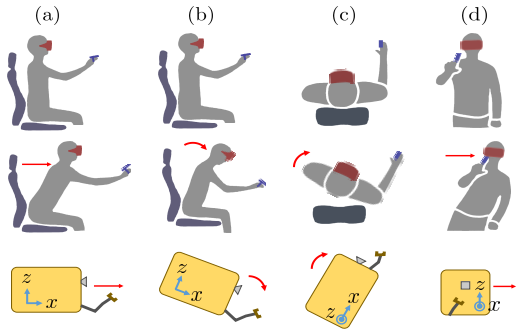

Fig. 4: Human torso motions on the actuated chair and their corresponding ROV motions: a) translation forward; b) pitch rotation; c) yaw rotation; and d) sway to side.

The human torso motion is defined as a relative position and orientation of the body fixed frame $\{\mathcal{B}\}$ w.r.t the chair frame $\{\mathcal{D}\}$. In addition, we set a small thresholds to filter out small unintended human torso motion. Combining these, we can then express the torso-ROV mapping as

$$\begin{aligned} &\text{if } \|q_{db}\| \leq \epsilon_1, && v_{or}^b \rightarrow \lambda_1 q_{db} \\ &\text{if } |3 - \text{tr}(R_{db})| \leq \epsilon_2, && \omega_{or}^b \rightarrow \lambda_2 \tilde{\omega}_{db} \end{aligned} \tag{3}$$

where, λ_1 and λ_2 are some scalar scaling factors, $\text{tr}(\star)$ is trace of the matrix $\star$, ϵ_1 and ϵ_2 are some scalar thresholds for filtering out user's small unintended motion. Here, note also $\tilde{\omega}_{db}$ is not an actual angular velocity but the rotational axis (twist) defined by $R_{db} = e^{\omega_{db} t}$ where, $\|\tilde{\omega}_{db}\| = 1$ and $t \in \mathfrak{R}$ is a real number. Initially, we set $q_{db}(0) = 0$, and $R_{db}(0) = I$. We also set $[q_{db}]_z = 0$ and $[\tilde{\omega}_{db}]_x = 0$ where the notation $[\star]_x$ is the x-axis component of the vector $\star$. We define body x-axis as forward/backward direction and z-axis as upward/downward direction. Here we have, $[q_{db}]_z = 0$, because the user cannot generate the upward/downward motion naturally on the chair. $[\tilde{\omega}_{db}]_x = 0$ is because we prevent the ROV's rolling motion. Although the above motion mapping omits the z-directional translation, the user can still intuitively operate the ROV like a nonholonomically constrained vehicle by using pitch, yaw, and forward/backward translation so that operator can reach any height.

3) Hand vs. End-effector: It is clear that if the master wants to grip an object in their view by using actual hand motion, the best way is to coordinate the manipulator end-effector pose with the human hand motion. We can express

this control objective s.t.

$$\begin{pmatrix} q_{rt} \\ R_{rt} \end{pmatrix} \rightarrow \begin{pmatrix} \lambda_3 q_{bh} \\ R_{bh} \end{pmatrix} \tag{4}$$

where, λ_3 is a scaling factor due to the different sizes of the human arm and manipulator. Please note that we map the 'relative' pose between the user's body and hand to the manipulator end-effector pose relative to the ROV. By doing so, even if a human moves his/her torso to control the ROV platform, the manipulator keeps its relative pose w.r.t the ROV unless the user moves their hand.

In addition, we assume that the end-effector is equipped with a gripper with only one DOF, open and close, with two rigid fingers as typical for most commercial ROV-manipulators. With this end-effector, dexterity of the human fingers cannot be fully realized due to the lack of DOF. Thus, we only map the tip pinch motion between the index finger and thumb onto the gripper motion. Note that we do not use distance between the index finger and thumb which may appear more natural for motion of the gripper. Instead, we use the flexion angle of the index finger (relative angle of the index finger w.r.t the back of human hand) onto the gap of the gripper. This is because flexion motion of the index finger dominates the pinch motion and the angle is practically easier to measure than the distance. We then linearly map the scaled angle to the distance of the gripper.

B. Slave Robot Autonomous Control

To realize the above whole-body tele-command mapping (2)–(4) in Sec. III-A, we design control input (1). For feedback control, we assume that all necessary state information can be obtained by using appropriate sensors such as IMU, dopper velocity meter, joint encoders, etc.

1) Camera Rotation control: The control input of camera motion is body angular velocity of the camera ω^b_{rc}. One possible control design to achieve $R_{rc} \rightarrow R_{be}$ is as follows

$$\omega^b_{rc} = R^T_{be} R_{rc} - R^T_{rc} R_{be} \tag{5}$$

2) ROV Platform Control: As mentioned in Sec.III-A.2, the human user operates the ROV with their torso motion. For this, the mapping is not positoin-positoin, but position-velocity. This then implies that we do not need a precise pose control of ROV platform, as some pose error will be easily correct by the user's maintaining a command motion. At the same time, due to the large inertia and drag with limited thrusts, the ROV platform itself often possesses a slow dynamics. Now, to achive the desired motion of the ROV as defined in (3) while considering these aspects, we define the ROV platform control s.t.,

$$\begin{bmatrix} v^b_{or} \\ \omega^b_{or} \end{bmatrix} = \mathrm{LPF} \begin{bmatrix} \lambda_1 q_{db} \\ \lambda_2 \tilde{\omega}_{db} \end{bmatrix} \tag{6}$$

where LPF is low pass filtering to take into account the ROV platform's slow dynamics. This means that even though human motion command is fast, the ROV will follow only the low frequency motion.

3) Manipulator Motion Control: In order to achieve the last teleoperation command (4), we define body velocity of the end-effector w.r.t the ROV as

$$V^b_{rt} = \begin{bmatrix} v^b_{rt} \\ \omega^b_{rt} \end{bmatrix} = \begin{bmatrix} R^T_{rt} \dot{q}_{rt} \\ (R^T_{rt} \dot{R}_{rt})^\vee \end{bmatrix} = \begin{bmatrix} R^T_{rt} \left[\dot{q}^d_{rt} - k(q_{rt} - q^d_{rt}) \right] \\ R^T_{bh} R_{rt} - R^T_{rt} R_{bh} \end{bmatrix}$$

where, $k \in \mathfrak{R}_+$ is control gain and $q^d_{rt} = \lambda_4 q_{bh}$ in (4). However, because V^b_{rt} is not a control input, we will find joint velocity of the manipulator to satisfy the equation (7) while respecting the manipulator limits, i.e. joint and joint velocity limits.

From the kinematics, we can define Jacobian relationship between joint velocity and the body velocity in $SE(3)$

$$V^b_{rt} = J^b_{rt} \dot{\theta} \tag{7}$$

where $J^b_{rt} := [J_v; J_w] \in \mathfrak{R}^{n \times 6}$ is body manipulator Jacobian. If the teleoperation command is feasible, the joint velocity can be $\dot{\theta} = {J^b_{rt}}^\dagger V^b_{rt}$ where $A^\dagger$ is pseudo inverse of matrix A. However, if the command is infeasible, we should find an optimal solution which is as close to the command as possible.

We assume that the manipulator has 6-DOF as so most commercial ROV-manipulator systems. Thus, our system is not redundant. If the command is infeasible due to the constraints, 6-DOF desired configuration cannot be achieved. In this case, the human perception of the usability decreases because the manipulator does not follow the operator's command.

Our approach is to prioritize the subset of the command which is more important to the human usability. We empirically find that the position error is more critical to the usability (the ease of use) than orientation error of the end-effector. In other words, human users seem more sensitive to the position error than the orientation error.

Based on this observation, we reformulate the Jacobian problem (7) as a hierarchical optimization problem by prioritizing the command. Since each control objective is 3-DOF, the 6-DOF manipulator becomes redundant w.r.t the first translation control objective. This can be formulated into the following lexicographic constrained optimization problem:

$$\begin{aligned} \text{lex} \min_{\dot{\theta}} \quad & \{\|J_v \dot{\theta} - v^b_{rt}\|, \|J_\omega \dot{\theta} - \omega^b_{rt}, \|\} \\ \text{subj.to} \quad & \dot{\theta}_{i,\min} \leq \dot{\theta}_i \leq \dot{\theta}_{i,\max}, \qquad i = 1, \cdots, 6 \end{aligned}$$

where $\dot{\theta}_{i,\max} = \min\left(\overline{\dot{\theta}}_i,\ \frac{\overline{\theta}_i - \theta_{i,k-1}}{\Delta t}\right)$, Δt is a time step of control loop, $\dot{\theta}_{i,\min} = \max\left(\underline{\dot{\theta}}_i,\ \frac{\underline{\theta}_i - \theta_{i,k-1}}{\Delta t}\right)$, and $\overline{\star}$ and $\underline{\star}$ are upper bound and lower bound of the scalar value $\star$. In addition, lex $\min$ is lexicographic optimization, considering the priority of the objective functions. For this optimization problem, we can further obtain its closed-form solution as follows:

$$\begin{aligned} \dot{\theta}^* &= J^*_v v^b_{rt} + N^*_v \dot{\theta}^*_2 \\ \dot{\theta}^*_2 &= [J_\omega N_v]^* \left(\omega^b_{rt} - J_\omega J^*_v v^b_{rt}\right) \end{aligned} \tag{8}$$

where N^*_v is null space projection matrix of J^*_v.

Please note that we do not use general pseudo inverse but deploy damped least-square method [24] with adjusted damping factor to avoid singularity. From the point of view of a manipulator, the human motion command is arbitrary because it is not a planned trajectory. Since the manipulator

has different kinematics from that of the human arm, it is not easy for the user to give motion command which are free from singularity of the slave manipulator by itself. Therefore, we define damped Jacobian J_v^* in (8) s.t.,

$$J_v^* = ({J_v}^T J_v + \gamma^2 I)^{-1} J_v$$
$$\gamma^2 = \begin{cases} 0 & \text{when } \underline{\sigma} \geq \epsilon \\ \left[1 - (\underline{\sigma}/\epsilon)^2\right] \gamma_{max}^2 & \text{otherwise} \end{cases}$$

where γ is the adjustable damping factor, $\underline{\sigma}$ is minimum singular value of the Jacobian, ϵ is an user-define threshold and γ_{max} is the maximum value of the damping factor. Refer to [24] for more details. Finally, the i^{th} element of the optimal solution will be replaced by $\dot{\theta}_{i,\max}$ (or $\dot{\theta}_{i,\min}$) if the element is lager (or less) than the maximum (or minimum) value.

C. Multi-Modal Feedback Design

1) Visual Feedback: Although visual information is the most important information for a remote operator as stated in Sec. I, conventional visual feedback displays such as computer screen does not provide the depth information and it is hard to feel the sense of reality. Thus, we use a HMD to improve immersion and provide depth information to the user which is especially important for the manipulation and grasping tasks.

However, the mobility of the mobile-manipulator can induce motion sickness which is typically reported when human uses the HMD. More precisely, if the human only see the camera view of the moving mobile platform through the HMD without any physical motion sense (vestibular sense), then the user feels the motion sickness and performing teleoperatoin tasks become difficult. Therefore, for long-hours operation such as deep-see exploration, the motion sickness should be reduced, and, for that, we adopt the actuated chair to provide vestibular feedback as explained below.

2) Vestibular Feedback: The motion sickness occurs due to the sensory conflict. The human's eyes perceive the visual movement, however, vestibular sense does not catch that motion experience. To reduce this motion sickness, we develop the 1-DOF actuated chair which provides the ROV's rotational motion to the human user (only yaw rotation in this research). Since the chair's rotational motion stimulates the vestibular sense, the user would feel less motion sickness. We performed user study to verify this - see the experimental results in Sec. IV.

3) Haptic Feedback: Since a kinesthetic haptic device like exoskeleton confines human motion, we deploy cutaneous haptic device which can provide tactile feedback and is also very light and portable. Worn on the index finger and the thumb, our cutaneous haptic devices provide contact force feedback to human user while the gripper of the manipulator makes a contact with an object. Since the human hand and the fingers are mapped into the manipulator and its gripper, cutaneous haptic device is expected to enhance user's realistic perception as if his/her fingers were the ROV-gripper.

In this paper, we only consider the case with the normal force in that the grasping motion of ROV-manipulator is 1-DOF. The normal desired force at contact, F_d, is designed according to the distance of index finger and thumb, x, as

$$F_d = \begin{cases} k\sqrt{x_c - x} + F_c & \text{when } x \leq x_c \\ 0 & \text{otherwise} \end{cases} \quad (9)$$

where k is constant coefficient, x_c is the distance of index finger and thumb at the moment of contact, and F_c is the minimum force at that moment. The force offset F_c is added in that human user needs the minimum threshold level of force to recognize whether a contact succeeded. The haptic feedback equation (9) is designed s.t., the user can sense a sharp increase of force in the early stage of contact and smooth increase of force in the latter stage.

We can then apply the desired force F_d to user's fingertip by controlling the rotation of motors. In order to do that, the relation between fingertip force and motor rotation angle is necessary. For this, we utilize the calibration result of the rotation angle to fingertip force based on the responses of human subjects as reported in [7].

IV. Experiment and User Study

A. System Setup

For our experiment, we utilize the master interface setup as shown in Fig. 2, each part of which is explained below.

1) Physics-Based Simulator: To verify our proposed multi-modal semi-autonomous teleoperation framework, we utilized simulator based on PhysX® for dynamic simulation and Ogre3D for 3D graphics (See Fig. 5). The dynamics model, which include 50,000 particles for generating buoyancy and drag forces, runs at 300 Hz with the graphics rendering-loop running at 40 Hz. This simulator was developed by Computer Graphics & Visualization lab of KAIST and provided to us for this research.

2) Motion Capture System: We used VICON® motion capture system to measure the human whole-body motion, which consists of 7 IR cameras with 200 Hz sampling time with millimeter scale resolution. To measure both the position and the orientation of the user's head, body, hand, finger, and the chair separately, markers were attached to the HMD, the subject's back, wrist, on the cutaneous haptic device, and on the chair.

3) HMD: We used the well-known commercial Oculus Rift® HMD, which has wide FOV (field of view) up to 90 degree, that is close to the human's FOV. The resolution is 1200×800 (640×800 per eye).

4) Actuated Chair for Vestibular Feedback: The actuated chair is equipped with a DC motor (100W, 38:1 gear ratio), which has an encoder with the resolution of 512 count/rotation attached to the motor shaft. For the feedback control of the chair, the control board measures the current rotation angle of the chair slightly slower than 1kHz.

5) Cutaneous Haptic Device: The device design is adopted from [6], which is actuated by two motors (Maxon DCX motor, $\phi = 10$mm, 3W, 16:1 gear ratio), each of which has encoder with the resolution of 1024 cnt/rev. Using US Digital® USB4 DAQ board and Arduino® board, the motor angles are measured and controlled in about 1kHz. The normal force to the user's fingertip is then produced by rotating the two motors in the opposite direction, while the shear force in the same direction.

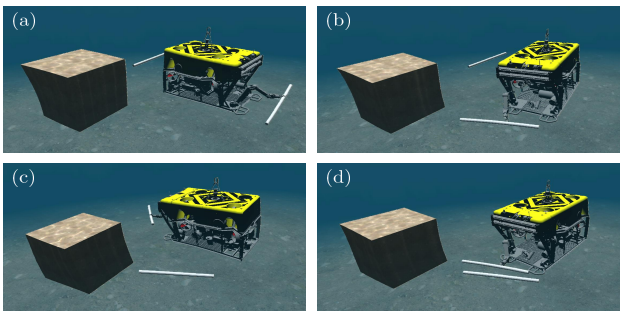

Fig. 5: User study task description: (a) Turning right and grasping, (b) Moving the cylinder, (c) Turning right and grasping, and (d) Moving the cylinder

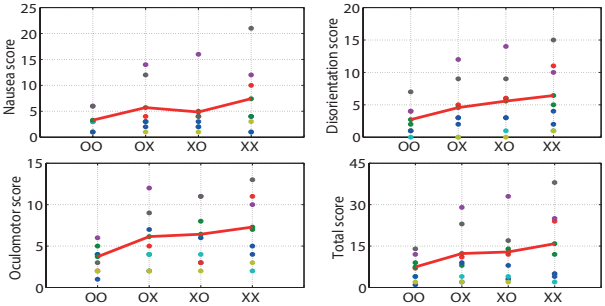

Fig. 6: Results of SSQ: each point represents the SSQ score of each participant and the red line represents their average value.

B. Human Subject Study

1) Experimental Setting: Subjects were seated on the actuated chair, wore the cutaneous haptic devices on their index and thumb fingers, and also HMD. They also wore earplugs to mask the motor noise. We tied the wires of the haptic device not to restrict the participants' motion.

2) Participants: 6 right-handed and 1 left-handed all male subjects with an age from 17 to 30 participated in this experiment. None of them had contributed to the design or the implementation of the experiment and had any known neurological disorders. The experiments were conducted in accordance with the Helsinki Declaration.

3) Objective and Procedure: Experimental task was designed to evaluate the effectiveness of our proposed teleoperation framework. To be more specific, we attempted to see if: 1) our semi-autonomous control can achieve more intuitive ROV-manipulator teleoperation with full visuo-haptic-vestibular feedback, 2) our cutaneous haptic device can provide an useful cue for the perception of the contact and grasping, and 3) the vestibular feedback can alleviate the HMD-induced motion sickness.

The experiment task is designed as follows (see Fig. 5): At the beginning, the subject can see one box and two cylinders placed horizontally through the HMD: The box is in front of the ROV, one cylinder is at the very left of the ROV, and the other is at its right side. The subject rotates the ROV by using his/her torso motion and grasps one cylinder. After grasping the cylinder, the subject moves it to the front of the box by rotating the ROV again. Next, the subject does the same thing for the second cylinder which will be at the opposite side of the first cylinder.

Each subject performed one practice and four trials of the given task. Each trial differs according to the condition whether the feedback from the actuated chair and the cutaneous haptic device are given or not. We made a random sequence so that none of the subjects performed the same order of the trials. Before starting the experiment, subjects were guided to proceed the task as fast as possible. For each trial, a supervisor measured the completion time and the number of the grasping failure. In addition, another supervisor asked each subject to fill in a questionnaire with an one minute break. If the subject requested longer rest, we granted that. The questionnaire consists of two part: one is designed to assess the usefulness of the cutaneous haptic feedback; and the other is SSQ (simulator sickness questionnaire) [25], which is a standard questionnaire to measure the simulator (motion) sickness. The SSQ is deployed to verify efficacy of our vestibular feedback.

4) Results and Discussion: The first questionnaire consists of 10 questions. Subjects responded to each question with a score based on 7-point Likert scale, where 1 represents a "complete disagreement" and 7 represents a "complete agreement" with the given statement. Among the 10 questions of our own questionnaire, we introduced two questions, which are associated with the manipulation task. We asked difficulty (or easiness) of grasping and moving the object: "Q7. It was difficult to transfer cylinders from one side to the other." and "Q9. It was easy to grasp the cylinders." The average scores are presented in the Table I, with the 'OX' symbols there identifying the four cases: with both the vestibular and the cutaneous haptic feedback (OO), vestibular but no cutaneous feedback (OX), cutaneous feedback but no vestibular (XO), neither vestibular nor cutaneous haptic feedback (XX). As can be seen from the Table I, the subjects reported that the easiest case was when they performed the grasping while receiving both the cutaneous haptic feedback and the vestibular feedback (OO). Please note here that Q7 is a negative types of question, whereas Q9 is a positive types of question.

	OO	XO	OX	XX
Q7	2.0	2.29	4.0	3.57
Q9	5.29	4.29	3.00	4.00

TABLE I: Average scores of difficulty of manipulation

We also deployed the SSQ to measure the motion sickness during the task. Fig. 6 shows that SSQ score increased when there was no vestibular feedback. The scores also said that the three symptom clusters of the human, nausea, disorientation, and oculomotor, were all ameliorated by using the vestibular feedback, confirming that the combination of suitable feedbacks can indeed reduce the HMD-induced motion sickness.

To check the learning effect, we also measured completion time and the number of the grasping failure in each order of the trials as shown in Table II. If participants adapted themselves to the interface as the number of the trials increases, the completion time and/or the number of failure are expected to decrease. Such is not evident from Table II, suggesting that the learning effect were negligible.

	1st	2nd	3rd	4th
Completion time	60.00	57.57	66.57	57.43
No. of failure	2.29	2.29	3.29	3.86

TABLE II: Average measurements in each trial

We also computed the average completion time and the number of failures for each feedback case and present them in Table III. As can be seen there, the first case ('OO', both haptic and vestibular feedback) ranks the best among the four cases. However, we could also observe the negative effect of single feedback (as shown in 'OX' and 'XO' cases in Table III) as compared to the no feedback case (i.e., 'XX'), which will be further investigated in our future publications. The video of the experiment is available at `http://www.youtube.com/watch?v=fOk2EM5UQLU`

	OO	OX	XO	XX
Completion time	51.71	71.14	64.29	54.43
No. of failure	2.00	3.71	3.86	2.14

TABLE III: Average measurements in each case

V. Conclusion

In this research, we propose a novel whole-body multi-modal semi-autonomous teleoperation framework for mobile-manipulator with the aim to minimize dexterity loss and information loss. First, the motion capture and whole-body motion mapping contactlessly measure the human motion and map this into the slave mobile manipulator. Next, slave robot autonomous control facilitates faithful command tracking, while considering the kinematic dissimilarity, slave robot's joint limit and singularity, with some priority. Last, we also design visuo-haptic-vestibular feedback with HMD, cutaneous haptic device, and actuated chair to minimize loss of information and reduce HMD-induced motion sickness. To verify the efficiency of the visuo-haptic-vestibular feedback, we performed some preliminary user study. The results show that the haptic-vestibular feedback not only improves system performance but only reduces the HMD-induced motion sickness.

As future work, we plan to develop the slave robot autonomous control with more rigorous consideration about human perception. In addition, the actuated chair is currently under-development of 2-DOF motion generation. Future works also include improvement of the whole-body motion mapping.

Acknowledgment

The authors would like to thank Professor Jinah Park and her team in KAIST for providing the simulator.

References

[1] R. Anderson and M. W. Spong. Bilateral control of teleoperators with time delay. *IEEE Transactions on Automatic Control*, 34(5):494–501, 1989.

[2] D. A. Lawrence. Stability and transparency in bilateral teleoperation. *IEEE Transactions on Robotics and Automation*, 9(5):624–637, 1993.

[3] Ryu Jee-Hwan, Kwon Dong-Soo, and B. Hannaford. Stable teleoperation with time-domain passivity control. *IEEE Transactions on Robotics and Automation*, 20(2):365–373, 2004.

[4] Lee Dongjun and M. W. Spong. Passive bilateral teleoperation with constant time delay. *IEEE Transactions on Robotics*, 22(2):269–281, 2006.

[5] D. J. Lee and K. Huang. Passive-set-position-modulation framework for interactive robotic systems. *IEEE Transactions on Robotics*, 26(2):354–369, 2010.

[6] K. Minamizawa, S. Fukamachi, H. Kajimoto, N. Kawakami, and S. Taichi. Gravity grabber: wearable haptic display to present virtual mass sensation. In *ACM SIGGRAPH: Emerging Technologies*, pages 250–258, 2007.

[7] Inyoung Jang and Dongjun Lee. On utilizing pseudo-haptics for cutaneous fingertip haptic device. In *Proc. IEEE Haptics Symposium*, pages 635–639, 2014.

[8] JT Reason. Motion sickness adaptation: a neural mismatch model. *Journal of the Royal Society of Medicine*, 71(11):819, 1978.

[9] Dongjun Lee, Oscar Martinez-Palafox, and Mark W Spong. Bilateral teleoperation of a wheeled mobile robot over delayed communication network. In *Proc. IEEE Int'l Conf. on Robotics and Automation*, pages 3298–3303, 2006.

[10] Antonio Franchi, Cristian Secchi, Markus Ryll, HH Bulthoff, and Paolo Robuffo Giordano. Shared control: Balancing autonomy and human assistance with a group of quadrotor uavs. *IEEE Robotics & Automation Magazine*, 19(3):57–68, 2012.

[11] Lee Dongjun, A. Franchi, Son Hyoung Il, Ha ChangSu, H. H. Bulthoff, and P. R. Giordano. Semiautonomous haptic teleoperation control architecture of multiple unmanned aerial vehicles. *IEEE/ASME Transactions on Mechatronics*, 18(4):1334–1345, 2013.

[12] ChangSu Ha, Zhiyuan Zuo, Francis B. Choi, and Dongjun Lee. Passivity-based adaptive backstepping control of quadrotor-type UAVs. *Robotics and Autonomous Systems*, 62(9):1305 – 1315, 2014.

[13] Valiallah Mani Monajjemi, Jens Wawerla, Richard Vaughan, and Greg Mori. Hri in the sky: Creating and commanding teams of uavs with a vision-mediated gestural interface. In *Proc. IEEE/RSJ Int'l Conf. on Intelligent Robots and Systems*, pages 617–623, 2013.

[14] N. Nitzsche and G. Schmidt. A mobile haptic interface mastering a mobile teleoperator. In *Proc. IEEE/RSJ Int'l Conf. on Intelligent Robots and Systems*, pages 3912–3917, 2004.

[15] P. Malysz and S. Sirouspour. Task performance evaluation of asymmetric semiautonomous teleoperation of mobile twin-arm robotic manipulators. *IEEE Transactions on Haptics*, 6(4):484–495, 2013.

[16] Andrea Sanna, Fabrizio Lamberti, Gianluca Paravati, and Federico Manuri. A kinect-based natural interface for quadrotor control. *Entertainment Computing*, 4(3):179–186, 2013.

[17] Susumu Tachi, Kazuo Tanie, Kiyoshi Komoriya, and Makoto Kaneko. Tele-existence (i): Design and evaluation of a visual display with sensation of presence. In *Theory and Practice of Robots and Manipulators*, pages 245–254. 1985.

[18] Charith Lasantha Fernando, Masahiro Furukawa, Tadatoshi Kurogi, Sho Kamuro, Katsunari Sato, Kouta Minamizawa, and Susumu Tachi. Design of TELESAR V for transferring bodily consciousness in telexistence. In *Proc. IEEE/RSJ Int'l Conf. on Intelligent Robots and Systems*, pages 5112–5118, 2012.

[19] Martin Buss, Angelika Peer, Thomas Schauß, Nikolay Stefanov, Ulrich Unterhinninghofen, Stephan Behrendt, Jan Leupold, M Durkovic, and Michel Sarkis. Development of a multi-modal multi-user telepresence and teleaction system. *The Int'l Journal of Robotics Research*, 29(10):1298–1316, 2010.

[20] T. Hulin, K. Hertkorn, P. Kremer, S. Schatzle, Jordi Artigas, M. Sagardia, F. Zacharias, and C. Preusche. The dlr bimanual haptic device with optimized workspace. In *Proc. IEEE Int'l Conf. on Robotics and Automation*, pages 3441–3442, 2011.

[21] E. Olguin-Diaz, G. Arechavaleta, G. Jarquin, and V. Parra-Vega. A passivity-based model-free force–motion control of underwater vehicle-manipulator systems. *IEEE Transactions on Robotics*, 29(6):1469–1484, 2013.

[22] Jonghui Han and Wan Kyun Chung. Active use of restoring moments for motion control of an underwater vehicle-manipulator system. *IEEE Journal of Oceanic Engineering*, 39(1):100–109, 2014.

[23] H. Yang and D. J. Lee. Dynamics and control of quadrotor with robotic manipulator. In *Proc. IEEE Int'l Conf. on Robotics and Automation*, pages 5544–5549, 2014.

[24] Charles W Wampler. Manipulator inverse kinematic solutions based on vector formulations and damped least-squares methods. *IEEE Transactions on Systems, Man and Cybernetics*, 16(1):93–101, 1986.

[25] Robert S. Kennedy, Norman E. Lane, Kevin S. Berbaum, and Michael G. Lilienthal. Simulator Sickness Questionnaire: An Enhanced Method for Quantifying Simulator Sickness. *The International Journal of Aviation Psychology*, 3(3):203–220, 1993.